

UC Riverside

UC Riverside Previously Published Works

Title

Overproduction of stomatal lineage cells in Arabidopsis mutants defective in active DNA demethylation

Permalink

<https://escholarship.org/uc/item/9t52w99t>

Journal

Nature Communications, 5(1)

ISSN

2041-1723

Authors

Yamamuro, Chizuko
Miki, Daisuke
Zheng, Zhimin
[et al.](#)

Publication Date

2014

DOI

10.1038/ncomms5062

Peer reviewed



Published in final edited form as:

Nat Commun. ; 5: 4062. doi:10.1038/ncomms5062.

Overproduction of stomatal lineage cells in *Arabidopsis* mutants defective in active DNA demethylation

Chizuko Yamamuro¹, Daisuke Miki¹, Zhimin Zheng¹, Jun Ma¹, Jing Wang¹, Zhenbiao Yang^{1,2}, Juan Dong³, and Jian-Kang Zhu^{1,4,†}

¹Shanghai Center for Plant Stress Biology, Shanghai Institutes for Biological Sciences, Chinese Academy of Sciences, Shanghai 200032, China

²Center for Plant Cell Biology, Department of Botany and Plant Science, University of California, Riverside, CA 92521, USA

³Waksman Institute of Microbiology, Rutgers University, Piscataway, NJ, 08854, USA

⁴Department of Horticulture and Landscape Architecture, Purdue University, West Lafayette, IN 47907, USA

Abstract

DNA methylation is a reversible epigenetic mark regulating genome stability and function in many eukaryotes. In *Arabidopsis*, active DNA demethylation depends on the function of the *ROS1* subfamily of genes that encode 5-methylcytosine DNA glycosylases/lyases. ROS1-mediated DNA demethylation plays a critical role in the regulation of transgenes, transposable elements and some endogenous genes, but there have been no reports of clear developmental phenotypes in *ros1* mutant plants. Here we report that, in the *ros1* mutant, the promoter region of the peptide ligand gene *EPF2* is hypermethylated, which greatly reduces *EPF2* expression and thereby leads to a phenotype of overproduction of stomatal lineage cells. *EPF2* gene expression in *ros1* is restored and the defective epidermal cell patterning is suppressed by mutations in genes in the RNA-directed DNA methylation pathway. Our results show that active DNA demethylation combats the activity of RNA-directed DNA methylation to influence the initiation of stomatal lineage cells.

Introduction

A network of genes that regulates stomatal development in *Arabidopsis* has been identified and established as a model for addressing fundamental questions such as how specific cell lineages are initiated and established, how stem cell-like asymmetric divisions are temporally maintained, and how precursor cells ultimately differentiate into functional, mature structures^{1, 2}. Earlier studies have shown that three master *bHLH* genes, *SPEECHLESS (SPCH)*, *MUTE*, and *FAMA*, act sequentially in stomatal fate transition and

Users may view, print, copy, and download text and data-mine the content in such documents, for the purposes of academic research, subject always to the full Conditions of use:http://www.nature.com/authors/editorial_policies/license.html#terms

[†]To whom correspondence should be addressed: jkzhu@purdue.edu.

Contributions C.Y., D.M. and J-K.Z designed the experiments. C.Y., D.M., Z.Z., J.M. and J.W. performed the experiments. C.Y., J.D., Z.Y. and J.Z wrote the manuscript.

determination. The function of *SPCH* is especially important for the first step in initiation of stomatal lineage cells^{3,4}. Another important factor controlling the stomatal lineage cell population is *EPIDERMAL PATTERNING FACTOR 2 (EPF2)*. *EPF2* belongs to a family of plant-specific, cysteine-rich peptides that is secreted by the early-stage lineage cells and acts as a negative regulator in stomata formation^{5,6}.

ROS1 is a bifunctional 5-methylcytosine DNA glycosylase/lyase critical for active DNA demethylation in most tissues of Arabidopsis plants^{7,8}. *ROS1* and its two paralogs, *DEMETER-like 2 (DML2)* and *DEMETER-like 3 (DML3)*, are required for the prevention of DNA hypermethylation at thousands of genomic regions^{9,10,11}. Loss-of-function mutations in these enzymes cause transcriptional silencing of some transgenes and endogenous genes^{7,12}. Unlike another paralog, *DEMETER (DME)*, which is known to be critical for active DNA demethylation in the central cell and thereby for gene imprinting and endosperm development¹³, a developmental function has not been established for *ROS1*. In this study, we found that *ROS1* loss-of-function mutants have a defect in epidermal cell patterning that is strikingly similar to the *EPF2* loss-of-function phenotype. We further show that the promoter region of the *EPF2* gene in *ros1* mutants is hypermethylated, which leads to a dramatic decrease in its mRNA level. Our findings provide the first evidence that active DNA demethylation initiated by *ROS1* plays an important role in controlling the dispersed stem cell population, the stomatal lineage cells, in plant development.

Results

ros1 mutant epidermis has more stomatal stem cells

The loss-of-function mutants, *ros1-4* and *rdd (ros1-3 dml2-1 dml3-1)*, do not exhibit apparent developmental phenotypes at the whole-plant level¹¹. However, microscopic observation reveals that *ros1-4* has clusters of small cells in the leaf epidermis, as exhibited in the *epf2-1* mutant (Fig. 1a–d and Supplementary Fig. 1). The “small-cell-cluster” phenotype is more severe in the *rdd* triple mutant than in *ros1-4* (Fig. 1c, d and Supplementary Fig. 1), but the *ros1* mutation seems to be the major contributor to the phenotype in the *rdd* mutant. The number of small cells is > 3-times greater in *ros1-4*, *rdd* and *rdd-2 (ros1-4 dml2-2 dml3-2)* than in the Col wild type, although the numbers of stomata are not different in the 3-day-old seedlings (Fig. 1e). Like *ros1-4*, the *ros1-3* and *ros1-6* mutants also exhibit a “small-cell-cluster” phenotype (Supplementary Fig. 2). Furthermore, F1 progenies from *ros1-4* × *ros1-3* but not *ros1-4* × Col or *ros1-3* × Col display the mutant epidermal patterning phenotype (Supplementary Fig. 3), and the phenotype in *ros1-4* is largely rescued by expression of the wild type *ROS1* gene (Fig. 2a–c). Previous research showed that the clustered small cells in *epf2* are stomatal lineage cells, which express the *SPCH* gene⁶. Because of the similarity in phenotypes, we suspected that the clustered, small cells in the *ros1-4* epidermis could be stomatal lineage cells. We crossed the *ros1-4* mutant with the stomatal cell fate-marker lines *SPCHpro:nucGFP* and *MUTEpro:GFP*. *SPCH* is required for initiation of asymmetric cell division in stomatal development, and *SPCHpro:nucGFP* expression is mainly found in the early stomatal lineage cells³ (Fig. 3a). As expected, all of the small-cell-clusters in *ros1-4* have *SPCHpro:nucGFP* expression (Fig. 3b, c), demonstrating an enlarged population of stomata

precursors in *ros1-4*. In contrast, *MUTE* expression is required for termination of asymmetric cell division and promotes the transition to guard mother cells (GMC)⁴, and the expression of *MUTE_{pro:nucGFP}* is restricted to the meristemoids in the wild type Col (Fig. 3d). In *ros1-4*, only a portion of the small-cell-clusters has *MUTE* expression (Fig. 3e, f). The behaviors of the SPCH and MUTE markers are consistent with those found in *epf2*⁶. We also examined the cotyledons of 10-day-old *epf2-1*, *ros1-4*, *rdd* and *rdd-2* plants, and found that these mutants have a similar increase in the numbers of stomata compared with the wild type Col (Supplementary Fig. 4). Together, these results suggest that some of the cells in the small-cell-clusters are arrested before the GMC stage in *epf2-1*, *ros1-4*, *rdd* and *rdd-2* mutants. Therefore, like *epf2* mutations *ros1* mainly affects the specification of stomatal lineage cells but does not dramatically change the differentiation of these cells into GMC.

ros1* mutations cause silencing of *EPF2

Given the similarity in phenotypes of the *ros1* and *epf2* mutants, we next analyzed the *EPF2* expression level in *ros1-4*, *rdd*, and *rdd-2* mutants at the early seedling stage by quantitative RT-PCR. The results showed that *EPF2* expression is dramatically reduced in the *ros1-4* and *rdd* mutants relative to Col (Fig. 4a). Because DNA methylation in promoter regions usually decreases gene transcription, we suspected that the reduced expression of *EPF2* in *ros1-4*, *rdd* and *rdd-2* might result from a hypermethylation of the *EPF2* promoter DNA. We searched for the methylation status of the *EPF2* promoter from the DNA methylomes of *ros1-4* and *rdd* mutants¹⁰. The region upstream of the *EPF2* promoter has an 835-bp hAT-like transposable element (TE) insertion with high methylation in Col, *ros1-4*, and *rdd*. We found increased DNA methylation levels in *ros1-4* and *rdd* mutants relative to the wild type Col in the *EPF2* promoter immediately downstream of the TE insertion (Fig. 4b). Individual locus bisulfite sequencing confirmed that the *EPF2* promoter is hypermethylated at all cytosine sequence contexts (CG, CHG and CHH, where H is C, A or T) in *ros1-4*, *rdd* and *rdd-2* (Fig. 4c). These results strongly suggested that DNA hypermethylation at the *EPF2* promoter leads to the decreases in *EPF2* expression that could be responsible for the small-cell-cluster phenotype in *ros1-4* and *rdd* mutants.

We also performed qPCR analysis for *epf2*, *ros1-4*, *rdd*, and *rdd-2* to measure changes in gene expression associated with stomatal development. The results indicated that, in *epf2*, the genes involved in stomatal development, such as *SPCH*, *MUTE*, *TMM*, *SCRM/ICE1* and *ERL1*, are up-regulated in expression relative to Col (Fig 4a and Supplementary Fig. 5). Consistent with the phenotypic similarity between *epf2-1* and *ros1-4* as revealed by microscopic observations, similar up-regulation of these genes was also observed in *ros1-4*, *rdd*, and *rdd-2* mutants (Fig 4a and Supplementary Fig. 5).

The epidermal phenotype of *ros1* is dependent on SPCH

SPCH loss-of-function mutants lack stomata and have only jigsaw-puzzle-shaped pavement cells in their leaf epidermis^{3, 4} (Fig. 3h), which is nearly identical to those in *EPF2*-overexpression lines^{5, 6}. Previous genetic and biochemical studies showed a tight connection between *EPF2* and *SPCH*¹⁴. The perception of the EPF2 peptide by ERECTA is thought to activate a mitogen-activated protein kinase (MAPK) cascade that phosphorylates SPCH to

down-regulate its function¹⁵. Thus, EPF2 negatively regulates SPCH function at the early stage of stomatal development. If ROS1 regulates *EPF2* expression and if the strong reduction in *EPF2* gene expression is responsible for the small-cell-cluster phenotype in *ros1-4*, we would expect that the loss-of-function *spch-3* mutation to be epistatic to *ros1-4*. We crossed *ros1-4* with *spch-3* and generated *ros1-4, spch-3* (-/-, +/-) plants. Of the progenies of selfed *ros1-4, spch-3* (-/-, +/-) plants, 24.3% were of the *ros1-4, spch-3* (-/-, -/-) genotype and showed the *spch-3* phenotype (Fig. 3g-i and Table 1). The genetic analysis indicates that ROS1 acts upstream of SPCH in stomatal development.

EPF2* expression rescues the epidermal phenotype in *rdd

We next tested whether expression of *EPF2* could rescue the small-cell-cluster phenotype in the *rdd* mutant. We generated *rdd* plants carrying the dexamethasone (DEX)-inducible *EPF2* construct (*DEXpEPF2*). The seedlings of *DEXpEPF2* were germinated and grown on medium containing 2.5 or 25 μ M DEX. The control plants grown on medium without DEX showed the *rdd* mutant phenotype (Fig. 3j). However, DEX-inducible ectopic expression of the *EPF2* gene rescued the *rdd* mutant defect in epidermal cell patterning and small cell number (Fig. 3j-m). With a high concentration of DEX, part of the epidermis produced stomata free or low-density area as previously observed when *EPF2* was overexpressed^{5, 6} (Fig. 3l). These results clearly show that the reduced expression of *EPF2* was responsible for the small-cell-cluster phenotype in *ros1* and *rdd* mutants.

***EPF2* silencing and epidermal defect in *ros1* depend on RdDM**

Previous work showed that the *RD29Apro:luciferase* transgene silencing triggered by *ros1-1* can be suppressed by mutations in components of the RNA-directed DNA methylation (RdDM) pathway such as *NUCLEAR RNA POLYMERASE D1 (NRPD1)* and *HISTONE DEACETYLASE6 (HDA6)*¹⁶. We constructed the double mutants *nRPD1-3 ros1-4* and *hda6 ros1-4* and used them to test whether the small-cell-cluster phenotype, and *EPF2* silencing and promoter DNA hypermethylation in *ros1-4* are caused by RdDM. The *nRPD1-3* and *hda6* single mutants did not have significant epidermal defects (Fig. 5a, c). However, these mutations strongly suppressed the small-cell-cluster phenotype in the *ros1-4* epidermis, since the epidermal patterning of *nRPD1-3 ros1-4* and *hda6 ros1-4* are almost identical to those of the *nRPD1-3* or *hda6* single mutants (Fig. 5b, d, g). The *NRPD1* gene encodes the largest subunit of Pol IV, which is thought to act at an early step of the RdDM pathway leading to the biogenesis of 24-nt small interfering RNAs (siRNAs) that direct the *de novo* DNA methyltransferase DRM2 to methylate DNA at RdDM target loci (Supplementary Fig. 6a)^{17, 18}. Using small RNA Northern blot analysis, we detected 24-nt siRNAs in *ros1-4* as well as in Col with a probe from the *EPF2* promoter (Fig. 5j and Supplementary Fig. 7). The *nRPD1* mutation blocked the accumulation of the siRNAs in Col and in the *ros1-4* background (Fig. 5j). These results strongly suggest that the siRNAs are the initial trigger of *EPF2* promoter DNA hypermethylation in *ros1-4*. Furthermore, we crossed the DNA methyltransferase triple mutant *drm1-2 drm2-2 cmt3-11 (ddc)* and *ros1-4*, and constructed the *drm1-2 drm2-2 cmt3-11 ros1-4* quadruple mutant and the *drm1-2 cmt3-11 ros1-4* triple mutant. The epidermal patterns of *drm1-2 drm2-2 cmt3-11* triple mutant were relatively normal (Fig. 5e, g). The *drm1-2 cmt3-11 ros1-4* triple mutant still exhibited the small-cell-

cluster phenotype but the phenotype was not observed in the *drm1-2 drm2-2 cmt3-11 ros1-4* quadruple mutant (Fig. 5f, g, Supplementary Fig. 6b, c). The results indicated that the *drm2-2* mutation was responsible for the suppression of the small-cell-cluster phenotype in the *drm1-2 drm2-2 cmt3-11 ros1-4* quadruple mutant, which is consistent with DRM2 being the *de novo* methyltransferase in the RdDM pathway^{17, 18}. Consistent with microscopic observations, qPCR and bisulfite sequencing analyses showed that *EPF2* expression levels and DNA methylation status at all cytosine contexts in the *EPF2* promoter region in *nprp1-3 ros1-4*, *ros1-4 hda6* and *drm1-2 drm2-2 cmt3-11 ros1-4* mutants were restored to almost the same level as in *nprp1* and *hda6* single mutants or in the *drm1-2 drm2-2 cmt3-11* triple mutant (Fig. 5h, i). Taken together, these results strongly suggest that siRNA-triggered *de novo* DNA methylation through the RdDM pathway is responsible for the DNA hypermethylation of the *EPF2* promoter region and therefore for the downregulation of *EPF2* gene expression in the *ros1-4* mutant.

Discussion

In this study, we have provided strong evidence that ROS1-initiated active DNA demethylation is necessary for the expression of the *EPF2* gene. Due to the insertion of a hAT-like TE in the upstream region of *EPF2* promoter, DNA methylation tends to spread from the TE into *EPF2* promoter to cause silencing of *EPF2*. ROS1 ensures *EPF2* expression by erasing DNA methylation to control a proper population of stomatal lineage cells (Fig. 6a, b). The DNA methylation of *EPF2* promoter and silencing of *EPF2* are dependent on RdDM. Our results suggest that ROS1 opposes RdDM action to ensure *EPF2* expression (Fig. 6c). It was reported recently that low relative humidity triggers the methylation of *SPCH* and *FAMA* via RdDM^{19, 20}. It would be interesting to determine whether ROS1 may play a role in opposing the RdDM action on *SPCH* and *FAMA* under low humidity. It would also be interesting to investigate whether ROS1 function may be regulated by environmental and/or developmental cues. *DME*, another member of the ROS1 family of 5-methylcytosine DNA glycosylases/lyases¹³, is regulated by developmental cues since it is preferentially expressed in the central cell of the female gametophyte and in the progenitor of the endosperm²¹. The *DME*-mediated demethylation is necessary for genomic imprinting of the maternal allele of *MEDEA* and other genes in the endosperm^{20, 22, 23}. *DME* is also important for the genomic demethylation in vegetative nuclei of developing pollens^{24, 25, 26}. *DME*-mediated demethylation affects genes targeted by RdDM^{27, 28}. Initiation and maintenance of stem cell populations is important in all higher eukaryotes. Our study demonstrates that ROS1-initiated active DNA demethylation ensures the expression of *EPF2*, thereby is important for the size of the stomatal stem cell population in the leaf epidermis. Future research will determine whether active DNA demethylation may also be important for other stem cells in plants.

Methods

Plant materials

The following mutants and transgenic lines were described previously: *SPCHpro:nucGFP*⁵, *MUTEpro:nucGFP*²⁹, *drm1-2drm2-2cmt3-11 (ddc)*³⁰, *epf2-1*⁶ (SALK_102777), *spch-3*³

(SAIL_36_B06), *nripd1-3* (SALK_128428) *rdd1¹*. *rdd-2* is a triple mutant of *ros1-4* (SALK_045303), *dml2-2* (SALK_113573) and *dml3-2* (SALK_056440). *Arabidopsis* T-DNA insertion lines were obtained from the Arabidopsis Biological Resource Center (<http://www.arabidopsis.org>). The *hda6* mutant was kindly provided by Dr. Zhizhong Gong (China Agricultural University).

Construction of plasmid DNA

EPF2 (CDS) was inserted into the cloning vector *pTA7002* for inducible expression³¹. *ROS1pro:ROS1* was inserted into the cloning vector *pEARLEY GATE 301*³² for ROS1 complementation analysis.

Bisulfite sequencing

One hundred ng of total DNA was analyzed by sodium bisulfite genomic sequencing using the BisulFlash DNA Modification Kit (Epigentek; <http://www.epigentek.com/catalog/index.php>) according to the manufacturer's protocol. A 1- μ l aliquot of bisulfite-treated DNA was used for each PCR reaction. PCR was performed in a total volume of 20 μ l using ExTaq (Takara; <http://www.takarabiousa.com/>). Sequenced fragments were amplified with primers specific for each region (Supplementary Table 1). Amplified PCR products were subcloned into the pCRII-TOPO vector (Invitrogen; <http://www.invitrogen.com/site/us/en/home.html>) following the supplier's instructions. For each region, more than 20 independent clones were sequenced from each sample.

Microscopic observations

Expanding cotyledons were stained by FM1-43 (Invitrogen; T35356), and fluorescence was detected with an Olympus BX53 fluorescence microscope with a GFP filter. A Leica SP5 confocal microscope was used for observation of GFP and FM4-64 (Invitrogen; F34653). Imaging conditions were excitation at 488 nm and a collecting bandwidth at 500–540 nm for GFP, and excitation at 561 nm and a collecting bandwidth at 600–645 nm for FM4-64.

Small RNA Northern blotting

Total RNA was extracted from 2 g of 10-day-old seedlings, and the small RNA was enriched by PEG precipitation. A 30 μ g quantity of small RNA per lane was run on a 15% acrylamide gel and then transferred to Hybond-N+ membranes. Hybridization followed the manufacturer's instructions.

DNA methylome data

DNA methylome data (GEO accession GSE33071) were described previously¹⁰.

Supplementary Material

Refer to Web version on PubMed Central for supplementary material.

Acknowledgments

The work was supported by funding from the Chinese Academy of Sciences.

References

1. Pillitteri LJ, Torii KU. Mechanisms of stomatal development. *Annu Rev Plant Biol.* 2012; 63:591–614. [PubMed: 22404473]
2. Bergmann DC, Sack FD. Stomatal development. *Annu Rev Plant Biol.* 2007; 58:163–181. [PubMed: 17201685]
3. MacAlister CA, Ohashi-Ito K, Bergmann DC. Transcription factor control of asymmetric cell divisions that establish the stomatal lineage. *Nature.* 2007; 445:537–540. [PubMed: 17183265]
4. Pillitteri LJ, Sloan DB, Bogenschutz NL, Torii KU. Termination of asymmetric cell division and differentiation of stomata. *Nature.* 2007; 445:501–505. [PubMed: 17183267]
5. Hara K, et al. Epidermal cell density is autoregulated via a secretory peptide, EPIDERMAL PATTERNING FACTOR 2 in Arabidopsis leaves. *Plant Cell Physiol.* 2009; 50:1019–1031. [PubMed: 19435754]
6. Hunt L, Gray JE. The signaling peptide EPF2 controls asymmetric cell divisions during stomatal development. *Curr Biol.* 2009; 19:864–869. [PubMed: 19398336]
7. Gong Z, et al. ROS1, a repressor of transcriptional gene silencing in Arabidopsis, encodes a DNA glycosylase/lyase. *Cell.* 2002; 111:803–814. [PubMed: 12526807]
8. Agius F, Kapoor A, Zhu JK. Role of the Arabidopsis DNA glycosylase/lyase ROS1 in active DNA demethylation. *Proc Natl Acad Sci USA.* 2006; 103:11796–11801. [PubMed: 16864782]
9. Lister R, et al. Highly integrated single-base resolution maps of the epigenome in Arabidopsis. *Cell.* 2008; 133:523–536. [PubMed: 18423832]
10. Qian W, et al. A histone acetyltransferase regulates active DNA demethylation in Arabidopsis. *Science.* 2012; 336:1445–1448. [PubMed: 22700931]
11. Penterman J, et al. DNA demethylation in the Arabidopsis genome. *Proc Natl Acad Sci USA.* 2007; 104:6752–6757. [PubMed: 17409185]
12. Zhu J, Kapoor A, Sridhar VV, Agius F, Zhu JK. The DNA glycosylase/lyase ROS1 functions in pruning DNA methylation patterns in Arabidopsis. *Curr Biol.* 2007; 17:54–59. [PubMed: 17208187]
13. Gehring M, et al. DEMETER DNA glycosylase establishes MEDEA polycomb gene self-imprinting by allele-specific demethylation. *Cell.* 2006; 124:495–506. [PubMed: 16469697]
14. Torii KU. Mix-and-match: ligand-receptor pairs in stomatal development and beyond. *Trends Plant Sci.* 2012; 17:711–719. [PubMed: 22819466]
15. Jewaria PK, et al. Differential effects of the peptides Stomagen, EPF1 and EPF2 on activation of MAP kinase MPK6 and the SPCH protein level. *Plant Cell Physiol.* 2013; 54:1253–1262. [PubMed: 23686240]
16. He XJ, et al. NRPD4, a protein related to the RPB4 subunit of RNA polymerase II, is a component of RNA polymerases IV and V and is required for RNA-directed DNA methylation. *Genes Dev.* 2009; 23:318–330. [PubMed: 19204117]
17. Matzke M, Kanno T, Daxinger L, Huettel B, Matzke AJ. RNA-mediated chromatin-based silencing in plants. *Curr Opin Cell Biol.* 2009; 21:367–376. [PubMed: 19243928]
18. Zhang H, Zhu JK. Seeing the forest for the trees: a wide perspective on RNA-directed DNA methylation. *Genes Dev.* 2012; 26:1769–1773. [PubMed: 22895250]
19. Tricker PJ, et al. Low relative humidity triggers RNA-directed de novo DNA methylation and suppression of genes controlling stomatal development. *J Exp Bot.* 2012; 63:3799–3813. [PubMed: 22442411]
20. Tricker PJ, et al. Transgenerational, dynamic methylation of stomata genes in response to low relative humidity. *Int J Mol Sci.* 2013; 14:6674–6689. [PubMed: 23531533]
21. Gehring M, et al. DEMETER DNA glycosylase establishes MEDEA polycomb gene self-imprinting by allele-specific demethylation. *Cell.* 2006; 124:495–506. [PubMed: 16469697]
22. Choi Y, et al. DEMETER, a DNA Glycosylase Domain Protein, Is Required for Endosperm Gene Imprinting and Seed Viability in Arabidopsis. *Cell.* 2002; 110:33–42. [PubMed: 12150995]
23. Hsieh TF, et al. Genome-wide demethylation of Arabidopsis endosperm. *Science.* 2009; 324:1451–1454. [PubMed: 19520962]

24. Schoft VK, et al. Function of the DEMETER DNA glycosylase in the Arabidopsis thaliana male gametophyte. *Proc Natl Acad Sci U S A*. 2011; 108:8042–8047. [PubMed: 21518889]
25. Calarco JP, et al. Reprogramming of DNA methylation in pollen guides epigenetic inheritance via small RNA. *Cell*. 2012; 151:194–205. [PubMed: 23000270]
26. Ibarra CA, et al. Active DNA demethylation in plant companion cells reinforces transposon methylation in gametes. *Science*. 2012; 337:1360–1364. [PubMed: 22984074]
27. Vu TM, et al. RNA-directed DNA methylation regulates parental genomic imprinting at several loci in Arabidopsis. *Development*. 2013; 140:2953–2960. [PubMed: 23760956]
28. Zemach A, et al. The Arabidopsis nucleosome remodeler DDM1 allows DNA methyltransferases to access H1-containing heterochromatin. *Cell*. 2013; 153:193–205. [PubMed: 23540698]
29. Dong J, MacAlister CA, Bergmann DC. BASL controls asymmetric cell division in Arabidopsis. *Cell*. 2009; 137:1320–1330. [PubMed: 19523675]
30. Cao X, et al. Role of the DRM and CMT3 methyltransferases in RNA-directed DNA methylation. *Curr Biol*. 2003; 13:2212–2217. [PubMed: 14680640]
31. Aoyama T, Chua NH. A glucocorticoid-mediated transcriptional induction system in transgenic plants. *Plant J*. 1997; 11:605–612. [PubMed: 9107046]
32. Earley KW, et al. Gateway-compatible vectors for plant functional genomics proteomics. *Plant J*. 2006; 45:616–629. [PubMed: 16441352]

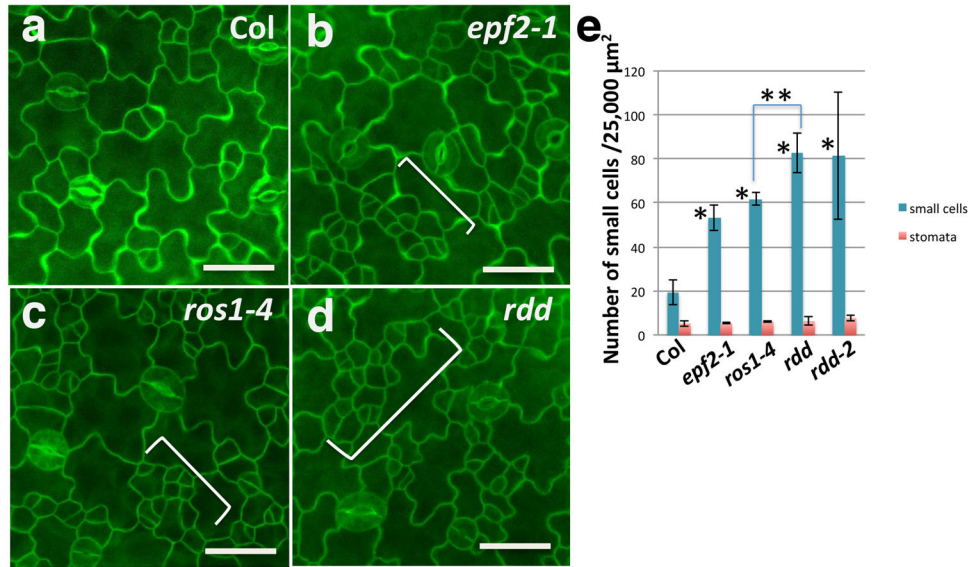


Fig. 1. Phenotypic analysis of epidermal patterning in the *ros1* and *rdd* mutants. **(a to d)** Microscopic image of cotyledon adaxial epidermal cells from 3-day-old Col **(a)**, *epf2-1* **(b)**, *ros1-4* **(c)** and *rdd* **(d)**. Small-cell-clusters are indicated by brackets. **(e)** Numbers of clustered small cells and stomata for Col, *epf2-1*, *ros1-4*, *rdd* and *rdd-2*. Values are means of \pm standard deviations per 25,000 μm^2 of 3-day-old cotyledon adaxial epidermis (n=3). Student-t, * $P < 0.03$ (significantly different from Col), ** $P < 0.02$. Images in **(a)** to **(d)** are at the same magnification. Scale bar, 30 μm .

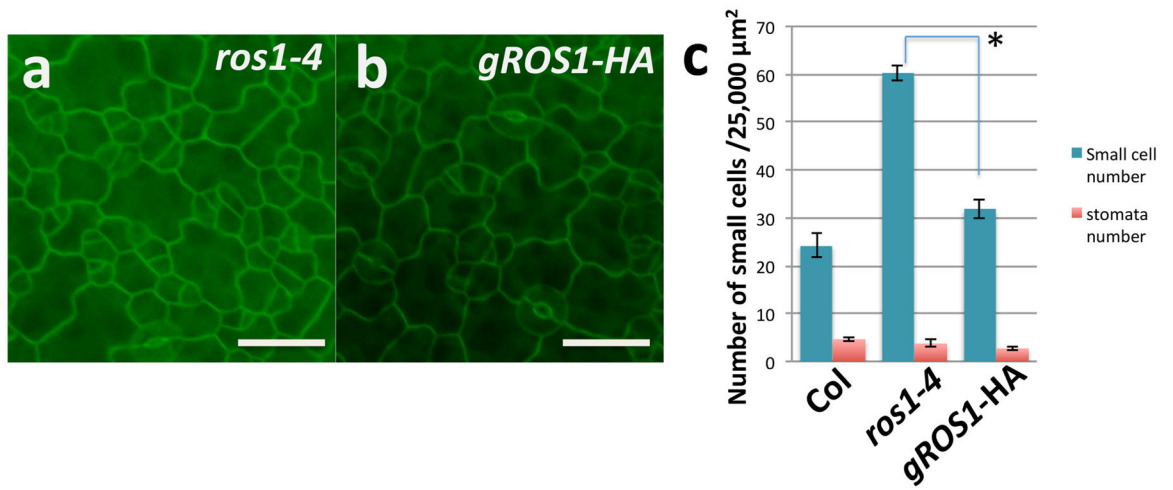
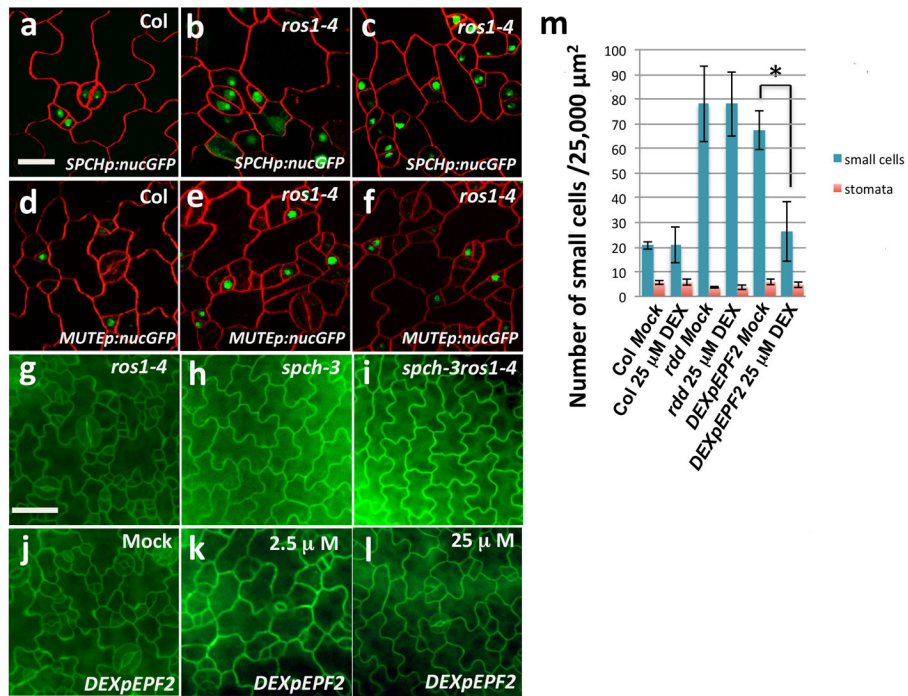


Fig. 2.

Complementation analysis of *ros1-4*. Cotyledon epidermal cell phenotype of 3-day-old seedlings of *ros1-4* (a) and *ros1-4* with *gROS1-HA* (b). The small-cell-cluster phenotype was rescued by expression of *gROS1-HA*. Scale bar, 30 μm . (c) Numbers of clustered small cells and stomata for Col, *ros1-4*, *gROS1-HA*. Values are means of \pm s.d. per 25,000 μm^2 of 3-day-old cotyledon adaxial epidermis (n=3). Student-t, * $P < 0.02$.

**Fig. 3.**

Expression of stomatal lineage reporter genes in *ros1-4* and genetic interactions between *ROS1*, *EPF2* and *SPCH* in epidermal patterning. **(a to f)** Confocal images showing expression of the stomatal lineage reporter genes *SPCH* and *MUTE* in adaxial epidermal cells of 3-day-old Col and *ros1-4* mutant seedlings. *SPCHp:nucGFP* **(a–c)**, *MUTEp:nucGFP* **(d–f)**. Arrow indicates a dividing cell. The genotypes are indicated above the images. Images in **(a)** to **(f)** are at the same magnification. Scale bar, 20 μm . **(g to i)** Genetic epistasis analysis of *spch-3* and *ros1-4*. **(g)** *ros1-4*, **(h)** *spch-3*, and **(i)** *ros1-4spch-3*. **(j to l)** Modulation of the small-cell-cluster phenotype in the *rdd* mutant by expression of DEX-inducible *EPF2* after treatment with **(j)** Mock (0 μM DEX), **(k)** 2.5 μM DEX, and **(l)** 25 μM DEX. Images in **(g)** to **(l)** are at the same magnification. Scale bar, 30 μm . **(m)** Numbers of clustered small cells and stomata for Col, *rdd* and the *rdd* mutant with DEX-inducible *EPF2* (*DEXpEPF2*) after treatment with Mock (0 μM DEX) or 25 μM DEX. Values are means of \pm standard deviations per 25,000 μm^2 of 3-day-old cotyledon adaxial epidermis (n=3). Student-t, * $P < 0.01$.

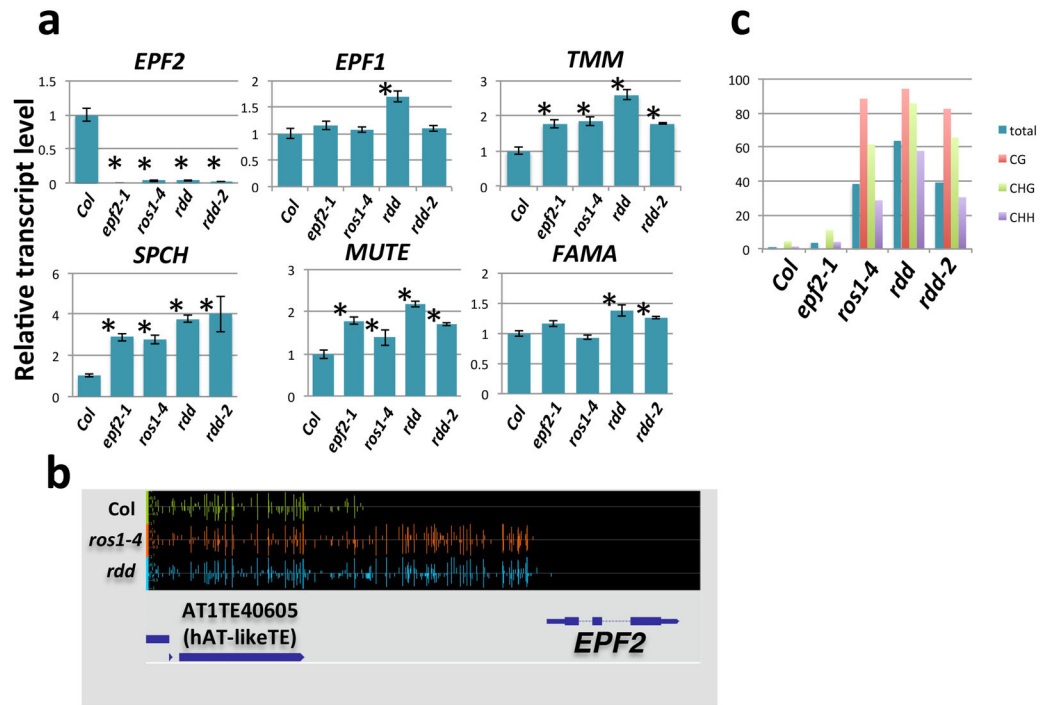
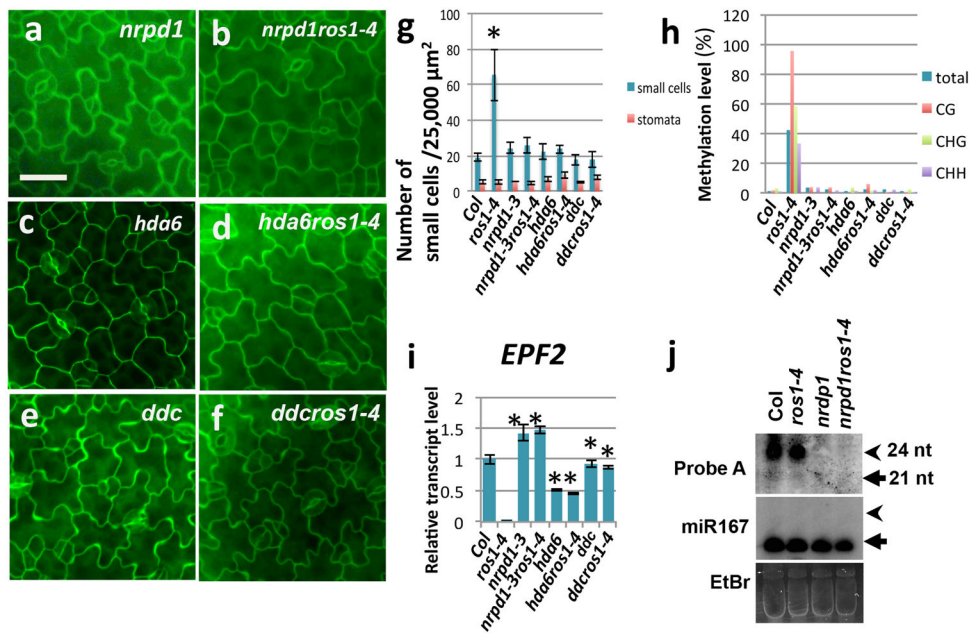
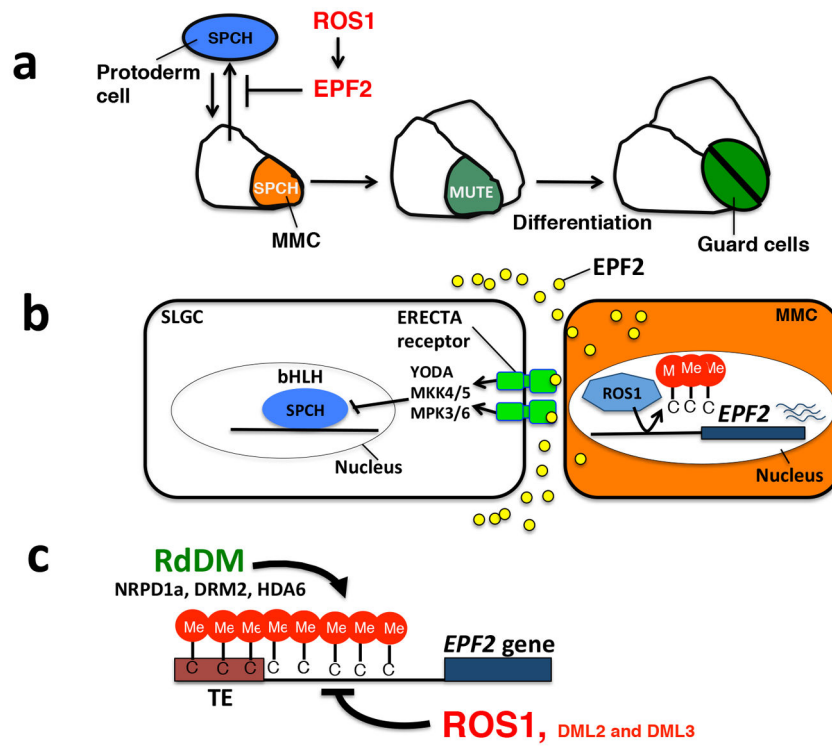


Fig. 4. *EPF2* expression and promoter DNA methylation. **(a)** Quantitative RT-PCR analysis of transcript levels of *EPF2* and other stomata-related genes in 3-day-old Col, *epf2-1*, *ros1-4*, *rdd*, and *rdd-2*. Error bars represent standard deviations (n=4). Student-t, * $P < 0.02$ (significantly different from Col). **(b)** Snapshot in the Integrated Genome Browser showing DNA methylation levels of the *EPF2* promoter and upstream region in Col, *ros1-4*, and *rdd*. **(c)** Bisulfite sequencing analysis of DNA methylation of the *EPF2* promoter in 3-day-old Col, *epf2-1*, *ros1-4*, *rdd*, and *rdd-2*.

**Fig. 5.**

Suppression of the *ros1* epidermal patterning phenotype by RdDM mutations. (**a** to **f**) Adaxial epidermal cell phenotype of 3-day-old seedlings. (**a**) *nrpd1-3*, (**b**) *nrpd1-3ros1-4*, (**c**) *hda6*, (**d**) *hda6ros1-4*, (**e**) *drm1-2drm2-2cmt3-13* (*ddc*), and (**f**) *drm1-2drm2-2cmt3-13ros1-4* (*ddcros1-4*). Images in (**a** to **f**) are at the same magnification. Scale bar, 30 μm . (**g**) Numbers of clustered small cells and stomata for Col, *ros1-4*, *nrpd1-3*, *nrpd1-3ros1-4*, *hda6*, *hda6ros1-4*, *drm1drm2cmt3* (*ddc*), *drm1drm2cmt3ros1-4* (*ddcros1-4*). Values are means of \pm standard deviations per 25,000 μm^2 of 3-day-old cotyledon adaxial epidermis (n=3). Student-t, * $P < 0.01$ (significantly different from Col). (**h**) Bisulfite sequencing analysis of the *EPF2* promoter, and (**i**) Quantitative RT-PCR assay of *EPF2* transcript levels in Col, *ros1-4*, *nrpd1-3*, *nrpd1-3ros1-4*, *hda6*, and *hda6ros1-4*, *drm1drm2cmt3* (*ddc*), *drm1drm2cmt3ros1-4* (*ddcros1-4*). Student-t, * $P < 0.01$ (significantly different from *ros1-4*). Error bars represent standard deviations (n=4). (**j**) Small RNA Northern blot analysis in Col, *nrpd1-3*, *ros1-4*, and *nrpd1-3ros1-4*. tRNA and other RNA bands stained with ethidium bromide (EtBr) were used as loading control. miR167 was detected as an internal control. Arrows and arrowheads indicate the positions of size markers, 21 nt and 24 nt, respectively.

**Fig. 6.**

A diagrammatic model of ROS1 function in stomatal development.

(a) A model for ROS1 function in stomatal development. ROS1 negatively regulates the entry into the stomatal lineage through *EPF2*. The bHLH protein SPCH is necessary for establishing the stomatal lineage. The bHLH protein MUTE is required for the termination of meristemoid asymmetric division and for the promotion of the GMC cell-state transition. (b) ROS1 removes DNA methylation from the *EPF2* promoter to enable expression of the *EPF2* gene, and EPF2 peptides are secreted outside of the meristemoid mother cell (MMC) to be received by the ERECTA receptor in the cell membranes of neighbor cells, SLGC (stomatal lineage ground cell). (c) ROS1 and RdDM antagonistically regulate the DNA methylation status of the *EPF2* promoter.

Table 1The segregation of the *spch-3* mutant phenotype

	Number	Percentage
<i>ros1-4</i>		
phenotype	56	75.68
<i>spch-3</i>		
phenotype	18	24.32
Total	74	100

The segregation of the *spch-3* mutant phenotype in the progeny of selfed *ros1-4, spch-3* (-/-, +/-) was close to the expected frequency of 25%.

Author Manuscript

Author Manuscript

Author Manuscript

Author Manuscript